Shubnikov–de Haas effect in KHg_x-graphite intercalation compounds

G. Timp, T. C. Chieu, and P. D. Dresselhaus
Department of Electrical Engineering and Computer Science, Massachusetts Institute of Technology, Cambridge Massachusetts 02139

G. Dresselhaus
Francis Bitter National Magnet Laboratory, Massachusetts Institute of Technology, Cambridge, Massachusetts 02139
(Received 28 November 1983)

The electronic structure of the KHg_x-graphite intercalation compounds near the Fermi surface is investigated by the Shubnikov–de Haas technique in magnetic fields up to 22 T and in the temperature range $1.5 < T < 27$ K. The experimental results for stages $n = 1$, 2, and 3 are consistent with a modification of the pristine graphite band structure which incorporates k_z-axis zone folding. This interpretation suggests that charge transfer to the graphite layers decreases in the potassium amalgam compounds as compared with the same stage potassium compounds. For selected cross-sectional areas the angular dependence and cyclotron masses are also measured and compared to the theoretical model. The qualitative agreement with the model suggests that in-plane zone folding could be important and that an accurate band calculation including graphite-intercalate interactions is necessary to fit the Shubnikov–de Haas periods.

INTRODUCTION

One of the most striking changes which occurs in intercalated graphite is the modification of the electrical properties from semimetallic to metallic behavior by intercalation.[1] These new electrical properties are associated with significant changes in the electronic structure in a material in which the structure of the graphite layers is essentially unchanged. The large electronic changes occur as a result of charge transfer to the graphite layer and also as a consequence of the more two-dimensional nature of the intercalation compound.

The measurement of magneto-oscillatory phenomena represents one of the most sensitive probes of the electronic structure of a metal near the Fermi energy. Almost all intercalation compounds thus far investigated show magneto-oscillatory phenomena as a result of the extremely high mobility associated with graphitic electrons. The lack of structural perfection in graphite-intercalation compounds (GIC's), in general, and of detailed band models for most compounds, makes the experimental data somewhat difficult to interpret quantitatively. Nevertheless, information regarding the electronic structure of GIC's has been gained from Fermi-surface measurements.[1] This paper reports measurements of Shubnikov–de Haas (SdH) oscillations in a commensurate intercalation compound (stage-1 KHg-GIC) which shows good intercalate layer order,[2] and which also shows interesting superconducting properties. Results for stages 2 and 3, which exhibit somewhat less structural order, are also presented.

The discovery of superconductivity in graphite intercalated with potassium-mercury alloys[3–6] (KHg_x-GIC's) has raised fundamental questions regarding the nature of superconductivity in these compounds, and the effect of changes in the stage on the superconducting properties. One fundamental question relates to whether the mechanism for superconductivity[7] involves a coupling between graphite π electrons and intercalate s and p electrons, as in the case of C_8K. A second question relates to why T_c for the stage-2 compound C_8KHg is larger than for the stage-1 compound C_4KHg.[3] Stage-1, -2, and -3 KHg_x-GIC's have been prepared,[6] and a superconducting transition has been observed in each stage compound. Iye and Tanuma[3] and Pendrys *et al.*[6] have observed that the transition temperature of the parent KHg_x material is enhanced with intercalation, and that the high anisotropy in the critical field, H_{c2}, and the relatively high superconducting transition temperatures of these GIC's ($T_c \sim 2$ K) both depend on the stage index. According to Iye and Tanuma,[3] the anisotropy ratio in H_{c2} increases from ~ 10 in the stage-1 KHg_x-GIC to ~ 25 in the stage-2 compound, while T_c increases from 0.92 K in the KHg alloy to a value in the range $0.8 < T < 1.4$ K in stage-1, 1.90 K in stage-2, and a value in the range $1.85 < T < 1.94$ K (Refs. 5 and 6) in the stage-3 intercalation compounds. The enhancement of T_c with intercalation and the increase of T_c with increasing stage index place constraints on the mechanism for superconductivity.[7]

The anisotropy and temperature dependence of the critical field, and the superconducting transition temperature, are related to the Fermi surface because the anisotropy in the critical field is directly dependent on the anisotropy of the superconducting gap function, while the gap and the transition temperature involve a convolution integral over the Fermi surface.

The anisotropy in the superconducting critical field H_{c2} has been given in terms of an effective-mass model[3] which therefore relates to the Fermi-surface and effective-mass measurements reported in this paper. Thus KHg_x-GIC's provide a unique opportunity to investigate the effect of variations in the Fermi surface (concomitant with the

change in the crystal structure) on the superconducting properties, because the crystal structure can be varied by changing the stage. Since quantum oscillatory phenomena directly yield the Fermi-surface cross-sectional areas, the Shubnikov—de Haas technique is particularly appropriate to an investigation of the carrier density, the number of equivalent carrier pockets, and their location in the Brillouin zone. Quantum oscillatory phenomena determine the extremal cross sections of orbits perpendicular to the direction of the magnetic field. Because of the c-axis anisotropy in GIC's, Fermi-surface topography studies are carried out as a function of the angle between the c axis and the magnetic field, and so, in principle, the volume of each carrier pocket is determined, and the charge transfer from the intercalate to the graphite layers can be determined. The anisotropy of the Fermi surface and the charge transfer have direct implications for the development of models for superconductivity in GIC's.[7]

Detailed calculations of the electronic structure in these compounds have not yet been reported. In the absence of such model calculations which would allow one to estimate the hybridization between the K and Hg s and p bands and the graphite π bands, one generally represents the electronic structure in terms of unhybridized bands with electron transfer between the graphite bands and the intercalate bands. This model leads to a somewhat oversimplified electronic band structure, but it serves as a valuable guide for the interpretation of experimental data.

Here we report the first observations of the Shubnikov—de Haas (SdH) effect in potassium-mercury GIC's for stages $n=1$, 2, and 3. The focus of this investigation is the development of approximate Fermi-surface models for these novel superconductors. The Fermi-surface topography was investigated by varying the angle between the magnetic field and the (001) crystallographic axis (c axis). In the stage-3 compounds, the cyclotron effective masses were derived from the measured temperature dependence of the amplitudes of the oscillations. The data are interpreted in terms of a phenomenological Brillouin-zone-folding model developed by Dresselhaus and Leung[8] (DL) for energy bands in GIC's. Their model is based on a Hamiltonian for a three-dimensional Fourier expansion of the graphite π bands[9] which accommodates the larger volume of the Brillouin zone assumed by the intercalation compound.

EXPERIMENTAL DETAILS

The samples used for this investigation were prepared from both highly oriented pyrolytic graphite (HOPG) and "kish" graphite host materials after the method of Hérold *et al.*[10] Kish graphite is a form of single-crystal graphite prepared by crystallization of carbon impurities from molten iron, and subsequently purified. The staging fidelity and homogeneity were evaluated by (00l) x-ray diffraction with the use of molybdenum $K\alpha$ radiation ($\lambda=0.7107$ Å). Based on (00l) scans, the samples were determined to be stage 1, stage 2, or stage 3 with a staging fidelity of better than 96%. The stage-1 and -2 compounds exhibited similar basal-plane $(2\times2)R0°$ order as evidenced by electron-diffraction measurements (in the temperature range $20<T<300$ K); that is, the basal-plane order is predominately $(2\times2)R0°$, although $(\sqrt{3}\times2)R$ (30°,0°) and $(\sqrt{3}\times\sqrt{3})R30°$ superlattices were frequently observed by electron diffraction. We recall that the commensurate intercalate order in the stage-1 compound has been shown to be extensive.[2] Extensive basal-plane intercalate order will augment the amplitude of SdH oscillations associated with both the intercalate and the zone-folded graphite in the stage-1 and -2 compounds. The basal-plane structure of the intercalate in the stage-3 compound is not well established, but preliminary work using electron diffraction indicates that the intercalate is incommensurate at room temperature.

The stoichiometries of the intercalant used for the preparation of compounds of different stages were KHg for stage $n=1$, KHg_2 for stage $n=2$, and $KHg_{2.5}$ for stage $n=3$.[2,11] However, the stoichiometry in the intercalation compound is significantly different from that of the intercalant, since it has been demonstrated that the potassium essentially intercalates the graphite completely before intercalation of the mercury is initiated.[10,11] For this reason an independent determination of the stoichiometry in the intercalation compound is desirable for the interpretation of Fermi-surface measurements.

A preliminary study of the stoichiometry of single-stage compounds similar to those used in these experiments was pursued by using Rutherford ion backscattering spectroscopy (RBS).[12] In the RBS measurement the ratios of the concentrations are of the three constituents derived from the relative height of the backscattered flux plotted as a function of energy. The results obtained from one stage-1 compound, one stage-2 compound, and one stage-3 compound show the following stoichiometries: the stage-1 compound yielded a stoichiometry of $C_3KHg_{0.77}$, for the stage-2 compound we found $C_7KHg_{0.72}$, and for the stage-3 compound we found $C_{13}KHg_{0.62}$. The error in the C:K ratio determination associated with the estimate of the relative height of the peaks is 50% in the stage-1 compound, 20% in the stage-2 compound, and 10% in the stage-3 compound, while the error associated with the determination of the K:Hg ratio in each case was less than 10%.

The typical dimensions of the intercalated HOPG-based samples were $3\times1.5\times0.1$ mm after cleaving perpendicular to the c axis in the inert argon atmosphere of a glove box. The kish-based specimens were irregularly shaped with dimensions on the same scale. Because potassium-amalgam GIC's were found to be air sensitive, the crystals to be tested were mounted onto the sample holder used for the SdH measurements inside a glove bag pressurized with argon gas. A conducting epoxy was used for electrical contact to the samples. The crystals were oriented with the c axis perpendicular to the direction of the current. After making electrical contact to the samples, the sample holder was loaded immediately into a cryostat, without exposing the samples to the ambient, and the cryostat was subsequently evacuated to $\sim10^{-5}$ Torr. For independent temperature control, the section of the cryostat containing

the samples was vacuum isolated from the liquid-^{4}He bath, but typically during the measurement, ^{4}He gas was condensed into the cryostat immersing the samples in liquid ^{4}He. The stage fidelity of the samples was evaluated through the use of (00l) x-ray diffraction following the SdH measurement, and we found no evidence for sample degradation as a result of the sample handling procedure.

The temperature was controlled by varying the vapor pressure over liquid ^{4}He in the temperature range $1.5 < T < 4.2$ K, and by using a varitemp Dewar for the range $2.0 < T < 26.0$ K. For precise temperature measurements in a magnetic field, a calibrated carbon glass resistor was used.[13]

The transverse magnetoresistance was measured as a function of the angle θ between the c axis of the KHg_x-GIC and the magnetic field vector, using the Montgomery four-terminal method.[14] Typically, the dc current, transverse to the field direction, was ~ 1 mA, and the voltage was detected by a Keithley model 140 dc amplifier. The measurements were performed at the Francis Bitter National Magnet Laboratory using either a 22- or 15-T magnet capable of sweeping the field range from zero field to the maximum field at variable rates. The design of the sample holder was such that the angle θ could be varied from $-90°$ to 90° while the samples remained essentially centered in the magnet. Expected variations in the magnetic field arising from variations in the sample position were less than $\pm 0.5\%$ of the total field. The angular dependence of the extremal cross sections observed in these compounds was determined by fixing the angle and sweeping the magnetic field. The angular dependence was calibrated against the known dependence of the SdH frequencies in a single-crystal graphite[15] specimen mounted adjacent to the KHg_x-GIC samples on the same sample holder. The error in the value of the absolute angle is estimated to be $\pm 2°$.

Magnetoresistance data were acquired by computer and the nonoscillatory component of the data was analyzed by fitting the magnetoresistance versus magnetic field H to a third-order polynomial in H. Because the data were fitted as a function of H, periodic errors in $1/H$ associated with the fit were minimized. The superconducting-to-normal transition occurring below 0.5 T was clearly evident in the resistance data, but was not studied in detail. The subtraction of the polynomial from a synchronized version of the data yields the oscillatory component of the magnetoresistance versus H, which is then arranged by using interpolation to monotonically and uniformly cover the same field range expressed as $1/H$. Since the oscillations in the resistance are periodic in $1/H$, the data record was analyzed using a standard discrete Fourier-transform algorithm to obtain the frequency spectra. The frequency plots given below for stages 2 and 3 show the variety of harmonic, sum, and difference frequencies (observed in more than one sample), and demonstrate the utility of the Fourier analysis in resolving the details of the spectra. The data record was digitally filtered to reduce side lobe contributions in the transform arising from the rectangular window function of the $1/H$ record. The digital filtering was accomplished by using either a Hamming or cosine window for the $1/H$ record.[16]

EXPERIMENTAL RESULTS

We have experimentally determined that the Fermi surface is stage dependent and the topography is, in general, anisotropic. Our first series of results demonstrates the dependence of the Fermi surface on the stage index.

Typical transverse magnetoresistance data taken as 1.5 K are shown in Fig. 1(a) for stage-1, Fig. 1(b) for stage-2, and Fig. 1(c) for stage-3 compounds. The data in each

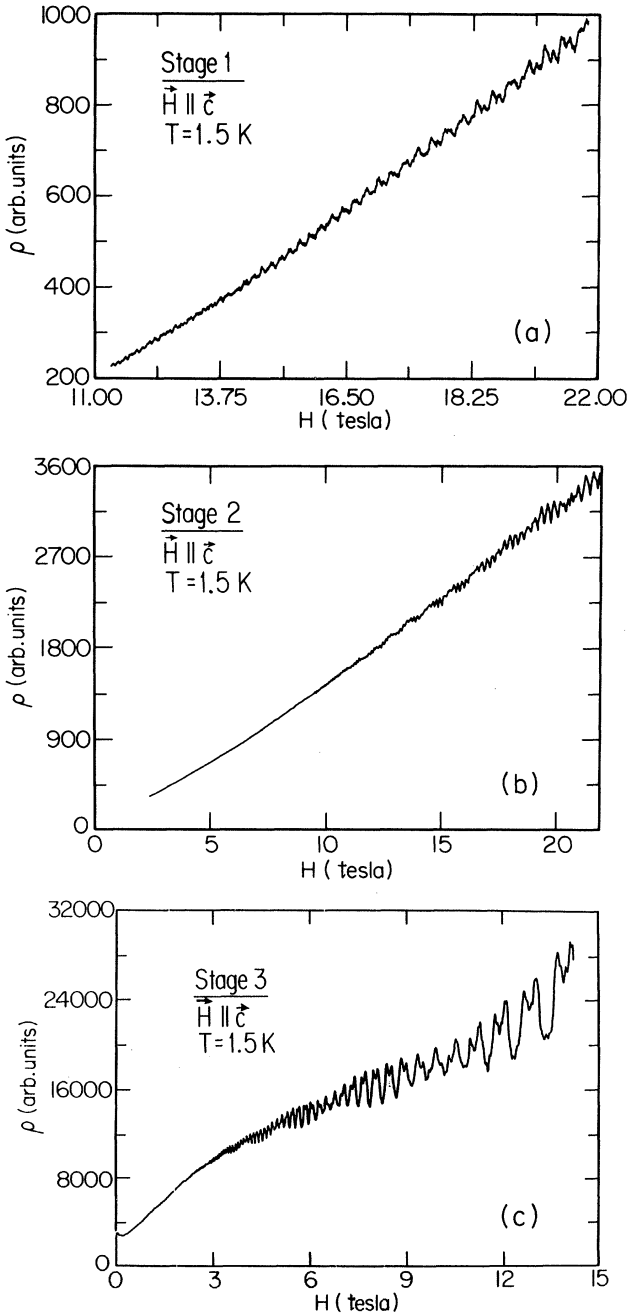

FIG. 1. Magnetoresistance plotted as a function of magnetic field ($\vec{H} \| c$ axis) for (a) stage-1 KHg-kish GIC, (b) stage-2 KHg_x-kish GIC, and (c) stage-3 KHg_x-HOPG GIC. Characteristic SdH oscillations dominate the high-field portions of each trace.

case show a quadratic dependence on H at low fields (<2.0 T) characteristic of closed orbits perpendicular to the field direction in a metal, while the quantum oscillations characteristic of a particular stage dominate the high-field region of every trace. It is noteworthy that the superconducting-to-normal transition could be routinely observed in the stage-2 and stage-3 samples as the magnetic field was swept through H_{c2}; the transition was observed in each case below 0.5 T [see, for example, Fig. 1(c)]. In the case of stage 3, the critical field ($H_{c2}\sim 0.2$ T) was found to be consistent with other measurements.[3,5,6]

In order to explicitly show the periodicity in $1/H$, we plot the Fourier power spectrum of the data of Fig. 1. The results are shown in Fig. 2(a) for stage-1, Fig. 2(b) for stage-2, and Fig. 2(c) for the stage-3 compound. The Fourier-intensity plot corresponds to an experimental trace with H along the c axis. The frequencies observed for the various stage compounds are tabulated in Table I. The magnetoresistance traces, the frequencies from which they are derived, and the angular dependence were reproducible and observed in two samples of stage 1, three samples of stage 2, and three samples of stage 3. In the stage-1 and stage-2 samples, frequencies larger than 1000 T are observed, while in the stage-3 specimens the highest frequency observed was 444 T. The spectra of Fig. 2 clearly show that several periodicities are present, and since the frequency of oscillation is directly proportional to an extremal cross section of the Fermi surface[17] through the relation $S_\alpha = 0.9546\times 10^{12}\ \Omega_\alpha\ (\mathrm{cm}^{-2})$, according to the tabulation in Table I, the corresponding extremal cross sections of the Fermi surface are stage depen-

TABLE I. Fermi-surface characteristics determined experimentally, and the predictions based on the Dresselhaus and Leung model (Ref. 8). The SdH frequencies are given in T and the cyclotron effective masses are in terms of the free-electron mass.

		Observed		Calculated	
Stage	Notation	Ω (T)	Mass	Ω (T)	Mass
1	Ω_γ	2490		2490	
	Ω_β	1090			
	Ω_α	52			
2	Ω_η	1490		1490	
	$\Omega_{\delta+\alpha}$	1284			
	Ω_δ	1250		1465	
	Ω_λ	1119			
	Ω_μ	901		502	
	Ω_γ	221		476	
	Ω_β	199			
	$\Omega_{2\alpha}$	50			
	Ω_α	28			
3	$\Omega_{\beta+\gamma}$	444	0.47		
	$\Omega_{\alpha+\gamma}$	308	0.40		
	Ω_γ	290	0.18	290	0.09
	Ω_β	155	0.14		
	$\Omega_{\beta-\alpha}$	137	0.40	108	0.06
	Ω_α	15	0.20		

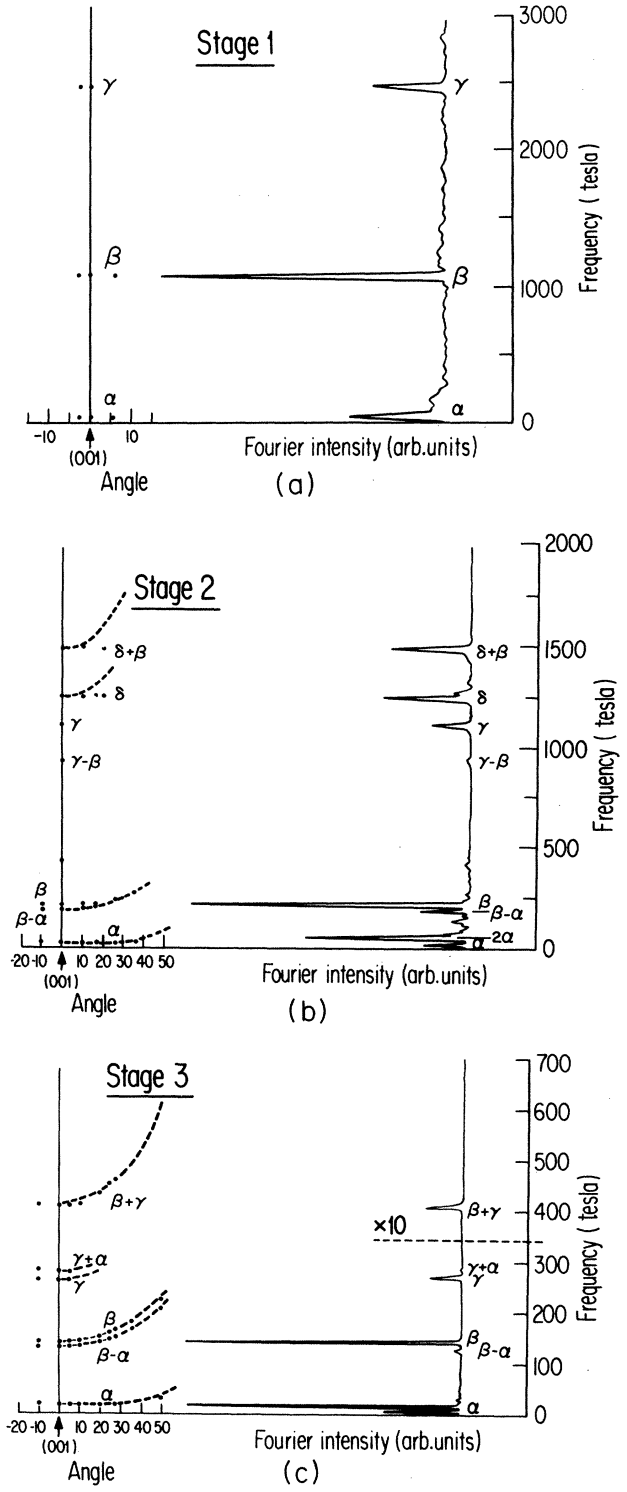

FIG. 2. Results for the Fourier transform of the oscillatory magnetoresistance (Fig. 1) for stages 1, 2, and 3 are shown in (a), (b), and (c), respectively. The dominant SdH frequencies are explicitly identified on each trace. Typical Fourier intensity plots corresponding to the condition where the magnetic field vector is aligned along the (001) crystallographic direction. For each of the dominant frequencies, the measured angular dependence (dots) is presented in the vicinity of the (001) direction. The dashed lines indicate the angular dependence corresponding to an idealized topography (see text).

dent. In the equation above, S_α denotes the extremal cross-sectional area, and the frequency Ω_α is in units of tesla.

In the stage-1 and stage-2 HOPG-based samples, high-frequency ($\Omega > 1000$ T) oscillations were severely damped[18] in contrast to corresponding kish-based specimens. The allowed orbits associated with either the intercalate or the graphite may be different near grain boundaries in HOPG-based samples, since, particularly for high-frequency oscillations, the cyclotron radius is approximately equal to the grain size ($r_c = 3000$ Å). We attribute the larger amplitude of the high-frequency oscillations observed in the kish-based compounds to the greater coherence of the crystal structure of kish graphite compounds relative to HOPG-based compounds.

We determined that the topography of the Fermi surface in KHg_x-GIC's is highly anisotropic (in direct correspondence with the crystal structure) by measuring angular dependence of the various frequencies observed in each stage compound. The results are summarized in Fig. 2. Because the amplitude of each oscillation decreases as a function of angle θ, the range of angle for which the SdH effect is observed was ultimately limited in each instance either by the signal-to-noise ratio or the topography of the Fermi surface. For the stage-1 specimens we were unable, with present methods, to observe the angular dependence of the frequencies beyond 6°; i.e., for $\theta > 6°$ we found a quadratic field dependence in the stage-1 compounds, but no resolvable SdH frequencies. For the stage-2 samples, anisotropy data were observed over the angular range $\theta < 50°$ in the frequencies 230 and 210 T, and the results are consistent with either a cylinder or a truncated ellipsoid in which the ratio of the major to minor axes, b/a, is greater than 3. The dashed lines through the data in Fig. 2(b) are indicative of the $1/\cos\theta$ dependence, characteristic of a cylindrical open Fermi surface. The higher frequencies observed in the stage-2 compound, 1490 and 1250 T, exhibited more isotropic behavior, as is evident by a comparison to a spherical model. However, over the limited range of angles for which we have data, the angular dependence could not be discriminated within experimental error from that of a cylinder [dashed line in Fig. 2(b)]. The stage-3 angular dependence results for the frequencies 444, 154, 137, and 15 T shown in Fig. 2(c) can be accommodated by either a cylinder [dashed line in Fig. 2(c)] or a highly anisotropic ellipsoid, $b/a > 3$. Generally, these results on stages 1, 2, and 3 are consistent with highly anisotropic Fermi-surface topographies, although because of the limited angular range for which we have data, we have not determined if the orbits perpendicular to k_z are open or closed orbits. We observed no resolvable frequencies for $\theta = 90°$, $\vec{H} \perp \vec{c}$.

For stage-3 compounds, we determined the temperature dependence of the amplitudes of oscillations observed in the magnetoresistance by using a ~15-T magnet. Because of the apparent number of harmonic, sum, and difference frequencies that were observed, the cyclotron effective mass was determined by the slope of the data compiled in the form $\ln(A/T^r)$ vs T where r is the order of the interaction[19] between frequencies identified as fundamental. The physical origin of the harmonic, sum, and difference frequencies was not investigated in this work. However, similar observations have been reported in other GIC's and have been related to magnetic breakdown or magnetic interaction effects.[19,20] The order of the interaction was assigned on the basis of measured values of the frequency and the amplitude. In the case of stage 3, we tentatively identified the 290-, 150-, and 15-T frequencies as fundamentals, and we have noted that 137 T ~ (150 − 15) T = 135 T, that 308 T ~ (290 + 15) T = 305 T, and that 444 T ~ (290 + 150) T = 440 T. For the case of both the harmonic and combination frequencies, the cyclotron effective masses associated with the corresponding frequencies will add. We found that it was possible to clearly observe the temperature dependence of the amplitudes for some frequencies over the temperature range $1.8 < T < 26$ K, as illustrated for selected temperatures in Fig. 3. The amplitude A was taken from the intensity found in the Fourier power spectrum where a filter was used to select a narrow range of magnetic fields, 0.15 T^{-1} wide. The measured amplitude was then associated with an average magnetic field value taken from the center frequency of the passband of the filter. The cyclotron mass is related to the slope s and value of magnetic field H through the formula

$$m^*/m_e = -\ln(A/T^r)/(rT)2\pi k_B m_e c = Hs/14.59 , \quad (1)$$

where H is given in T, k_B is the Boltzmann constant, c is the speed of light, and m_e is the free-electron mass. The amplitude data as a function of temperature are shown in Fig. 4(a) for the fundamentals and in Fig. 4(b) for the sum and difference frequencies that could be unambiguously resolved. The results are also tabulated in Table I. The effective masses associated with the sum and difference

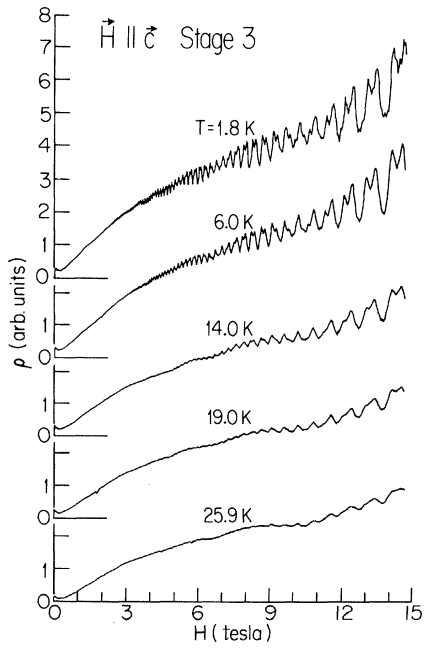

FIG. 3. Magnetoresistance as a function of field for a stage-3 KHg_x-HOPG sample at selected temperatures.

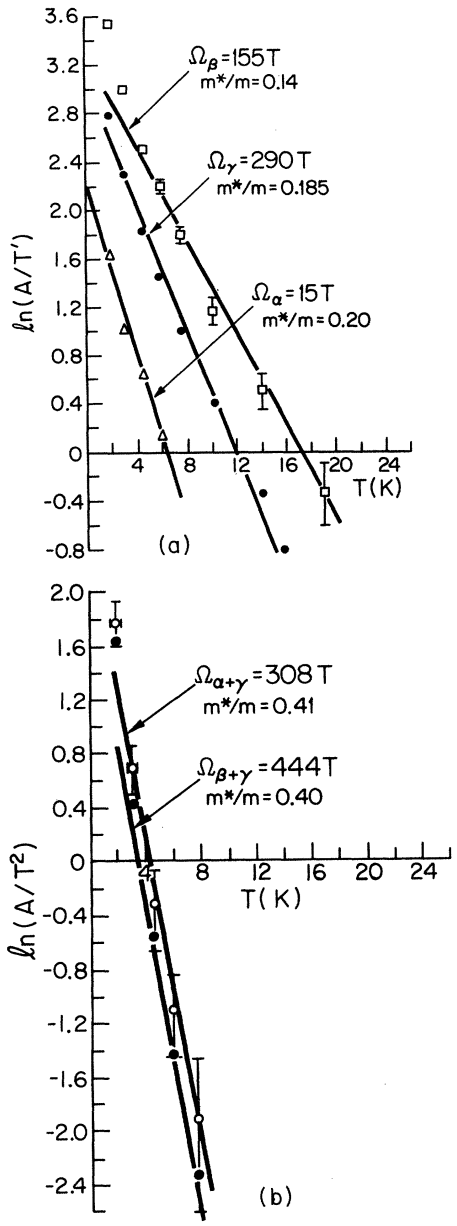

FIG. 4. Plot of $\ln(A/T^r)$ vs T, where A is the amplitude of SdH oscillations taken at a field of 10 T. The abcissa is labeled by the temperature T and r is the order of the oscillation. In (a) the cyclotron effective masses are identified with fundamental frequencies ($r=1$), while in (b) the masses are identified with sums of fundamentals ($r=2$). The slope of the least-squares-fitted line through the experimental points determines the mass, which is indicated on the figure along with the corresponding SdH frequency.

frequencies are found to be consistently higher than the values observed in frequencies identified as fundamentals. The cyclotron effective masses were obtained from two specimens, and were found to be consistent from sample to sample.

The cyclotron effective masses associated with the fundamental frequencies found in stage-3 compounds are consistent with either the effective masses observed in graphite-intercalation compounds,[21,22] or with cyclotron effective masses previously observed in crystalline mercury.[23] The masses associated with the sum and difference frequencies can be represented as a summation of the masses identified with the fundamental frequencies. For example, the effective masses corresponding to the frequencies 444 and 308 T are shown to be approximately equal to the sum of the cyclotron masses associated with the relevant fundamentals, supporting our identification of these frequencies as combination modes, i.e.,

$$m^*(444\text{ T})/m_e = 0.47 \sim m_\beta/m_e + m_\gamma^*/m_e$$
$$= 0.14 + 0.18 = 0.32\ ,$$
$$m^*(308\text{ T})/m_e = 0.40 \sim m_\alpha/m_e + m_\gamma^*/m_e$$
$$= 0.20 + 0.18 = 0.38\ .$$

The effective mass corresponding to the 15-T oscillation is sensitive to the polynomial fit used to remove the background magnetoresistance, and consequently the error associated with the mass determination is comparable to the magnitude of the mass.

Finally, in some cases, but not consistently, additional SdH frequencies were observed in samples designated as pure stage on the basis of an (00l) x-ray-diffraction characterization of the stage, suggesting the coexistence of two different stages. For example, in one stage-2 sample, in addition to the frequencies listed in Table I under stage 2, we found frequencies at 55, 1090, and 2500 T, characteristic of the stage-1 Fermi surface, and at 150 T, characteristic of the stage-3 Fermi surface. Similarly, in one stage-3 sample we observed frequencies at 230 and 1250 T, characteristic of the stage-2 compound. In each case the amplitudes corresponding to these oscillations were less than 2% of the peak amplitudes observed in the Fourier transform of the traces of the pure stage specimens, while the additional frequencies did not deviate more than 2% from the pure stage values. We conclude that the conventional (00l) x-ray-diffraction—characterization technique is an inadequate measure of the homogeneity of the staging order for SdH measurements, because the magnetoresistance measurement for homogeneous systems is sensitive to the bulk properties of the compound while molybdenum $K\alpha$ x-ray radiation has an extinction depth of only $\sim 35\ \mu$m (in stage-1 KHg-GIC's).

DISCUSSION

The basal-plane structure and basic symmetry of the graphite layers in KHg_x-GIC's are the same as in pristine graphite with approximately the same lattice constant, $a_0=2.46$ Å, and the basal-plane ordering of the intercalate is also reminiscent of the parent material.[10] The intercalate in stage-1 and -2 KHg_x-GIC's was first found by Hérold *et al.*[10] to be positionally commensurate to the adjacent graphite basal planes, and arranged in an hexagonal network where the unit vectors are twice that of graphite, a $(2\times2)R\,0°$ superlattice which corroborates our observations. Along the c axis, the thickness of the intercalate

layer, d_i, found in this work in the stage-1 compound ($d_i = 6.85$ Å) is identical to the value found in stage 2, while the value for d_i in the stage-3 compound is 5.7 Å. The ideal stoichiometry of the KHg_x-GIC's according to the structure proposed by Hérold *et al.*[10] is $C_{4n}KHg$. There are $8 \times n$ carbon atoms corresponding to a stage-n compound with a $(2 \times 2)R\,0°$ unit cell, but after Hérold[10] the multilayered structure of the intercalate has two potassium and two mercury atoms per primitive cell. The ideal stoichiometry for the stage-3 compound is not known; in the analysis we assumed for simplicity that the stoichiometry $C_{4n}KHg$ was also applicable to this stage.

In order to interpret the SdH data, we have applied the DL (Ref. 8) model for the electronic dispersion in GIC's. To accommodate the $(2 \times 2)R\,0°$ basal-plane superlattice, and the staging order in the stage-1 and stage-2 compounds, the Hamiltonian is zone-folded, and a unitary transformation, which preserves the eigenvalues of the Hamiltonian, maps the zone-folded Hamiltonian into a "layer" representation. For a stage-n compound in this model, n graphite layers are retained in the transformed Hamiltonian while the $(n+1)$st layer is transformed into an intercalate layer. In the simplest approximation used in this paper, the intercalate layer is then idealized as a "vacuum" layer which decouples the nearest-layer interaction between the bounding graphite layers and the "empty" intercalate layer.

To construct the Fermi surface from the dispersion relations, we first determined the Fermi energy according to the criterion that the largest experimentally observed extremal cross section identified with graphite be associated with the largest cross section about the K point in the model. According to the DL model, the number of cross sections and the corresponding frequencies depend on the Fermi level. To optimize the fit to the data in terms of the number of cross sections and the corresponding frequencies, a number of possible fits for the observed cross sections were investigated. The choices given below are not unique and do not reproduce all of the features of the data, but the choices were found to be consistent with the charge transfer estimate reported by Conard *et al.*[24] For economy in the analysis, the dispersion along the K-H direction was ignored, which implies that the Fermi-surface topography is cylindrical.

In the analysis of the data, we idealized the basal-plane structure of the intercalate in KHg_x-GIC's as being $(2 \times 2)R\,0°$, independent of the stage, and assumed a stoichiometry of $C_{4n}KHg$, although deviations from this "ideal" structure and stoichiometry were noted in the characterization of the specimens used in his work. The C:K ratio determined by RBS,[12] from one stage-1 sample, one stage-2 sample, and one stage-3 sample, agrees within experimental error with the stoichiometry proposed by Hérold *et al.*,[10] while the K:Hg stoichiometry does not agree with the "ideal" stoichiometry within the error. The differences observed in the stoichiometry may be attributed to either the variety of basal-plane structures observed in these compounds[2] or desorption of mercury as a result of improper handling. The difference in the structure and stoichiometry are particularly evident in the stage-3 compound in which the basal-plane order was observed to be incommensurate in one observation at room temperature, and the intercalate layer thickness d_i was found to deviate from the value found in stages 1 and 2 by 1.1 Å. In addition to the idealization of the structure of these compounds, we assumed that the experimentally observed extremal cross sections were located at the Brillouin-zone edge. This assumption has implications for the calculation of the charge density because of the multiplicity $(2\times)$ of carrier pockets associated with the zone edges. The multiplicity of carrier pockets arising from the identification of the SdH orbits with carriers at the zone edge augments the amplitude of the SdH oscillations. Since we were able to observe high-frequency oscillations, the observation itself implies that the high-frequency orbits are associated with the zone edges.

In Table I the values of the Fermi energy E_F and the extremal cross sections about the K point corresponding to the DL model are listed for each compound according to the stage index. The position in frequency of the extremal cross sections calculated on the basis of the DL model reproduce approximately some of the cross sections observed experimentally. It should be emphasized that except for the parameters in the Fourier expansion for the graphite π bands which have been justified by previous experimental work,[15] and our criterion for the identification of the Fermi energy, there are no adjustable parameters in the DL model.[8]

In our analysis of the results obtained from the stage-1 compounds, we identified the largest cross section observed at 2490 T with the only cross section predicted by the DL model. Because of the limited available angular range, the topography measured in stage-1 compounds did not discriminate between the cylindrical Fermi surface described in this model and, for example, a spherical topography possibly more characteristic of the intercalate. Two additional frequencies were identified at 1050 and 50 T, in the stage-1 compound, which are not accommodated in the DL model. If dispersion along the K-H axis and the stacking symmetry are included, other extremal cross sections at the K and H points can occur in the model, but the dispersion in zone-folded graphite is negligible with respect to the difference required to produce both the 2490- and the 1050-T orbits. Alternatively, if the 1050-T orbit is associated with the graphite, it is necessary to reexamine our initial hypothesis concerning the homogeneity of the $(2 \times 2)R\,0°$ phase (since for stage 1 there is only one graphitic carrier pocket according to DL). The interpretation of the 1050- and 50-T cross sections in terms of multiple basal-plane structure is appealing since multiphase coexistence has been observed in these compounds.[2] It is also possible that these SdH frequencies correspond to orbits associated with intercalate bands. The coherency of the structure of the intercalate layer may be sufficient in the stage-1 compound to support orbits with a cyclotron radius of $v_F/\omega_c = \sim 1000$ Å, where v_F is the Fermi velocity and ω_c is the cyclotron frequency. It has been shown[2] that the extent of the basal-plane structure of the intercalate is at least comparable to this value.

For the stage-2 compound, the number of orbits identified in the data is larger than that predicted by the DL

model. For the assignment shown in Table I, the 1284-T orbit was identified as the largest graphite extremal cross section. Based on this choice the predictions of the model yield orbits at 1254, 407, and 381 T, which are respectively identified with the 1250-, 221-, and 190-T frequencies observed experimentally. The angular dependence of the 1250-, 221-, and 190-T orbits are consistent with this interpretation within the experimental error. By noting that 1490 T$\sim$(1284+221) T and 28 T$\sim$(221−190) T, it is also possible to identify the 1490- and 28-T orbits as sum and difference frequencies in this interpretation corresponding to the fundamental frequencies identified in the DL model: 1284, 1250, 221, and 190 T. The discrepancy between the magnitude of the frequencies predicted by the model (407 and 381 T) and the frequencies observed experimentally in the stage-2 compounds (221 and 190 T) may be indicative of a strong hybridization of the graphitic and intercalate orbitals. The orbits observed at 1119 and 50 T are not identified with the chosen assignment and may be associated with either intercalate orbits or graphitic orbits arising from inhomogeneities in the superlattice order.

In the case of stage 3, the frequencies predicted from the DL model agree qualitatively with the identification of fundamental orbits made on the basis of the cyclotron-mass data. Using the 290-T orbit to fix the Fermi level, we subsequently identified the 108-T prediction with the 155-T frequency observed experimentally. However, the cyclotron effective masses obtained from the model according to the formula

$$m^* = (\hbar^2/2\pi)(\partial S/\partial E)_{E=E_F}$$

do not agree within the error of the measurement, suggesting that the graphitic and intercalate energy levels are hybridized.

The charge transfer per carbon atom f_C was estimated for each stage compound from the DL model by an integration over the volume of the Brillouin zone defined by the Fermi surface. Since the Fermi surface was defined to be cylindrical, the volume is determined by multiplying the extremal cross sections at the K point by the reciprocal-lattice vector $2\pi/I_c$. To obtain a value for f_C the result of the integration was divided by the product of the volume of the Brillouin zone corresponding to the superlattice and the number of carbon atoms per primitive unit cell. The results of the calculation are summarized in Table I.

Conard *et al.*[24] determined the charge transfer to the carbon layer for the ternary compounds C_4KHg and C_8KHg from the Knight shifts of the ^{13}C line. The values reported by Conard for the stage-1 and stage-2 compounds are $f_C(n=1)=-0.072$ and $f_C(n=2)=-0.040$, respectively, which are consistent with the predictions of the DL model of $f_C(n=1)=-0.063$ and $f_C(n=2)=-0.049$, respectively, based on the SdH data. The values for f_C listed in Table I indicate an abrupt change in the ionization of the intercalate in the stage-3 compound which may be due to the change in the structure and stoichiometry of the intercalate layer noted above.

The estimate given for the charge transfer and the calculation of the dispersion according to the simplest version of the DL model both assume no shift in the bounding layer potential. The approximation of a shifted bounding layer potential for the stage-3 compounds would allow the charge to be more localized on the bounding graphite planes.[25] However, in the limit that the charge transfer to the interior graphite layers is zero so that the number of carbon atoms in the calculation of the charge transfer is reduced, the charge transfer per carbon atom is only $f_C(n=3)=-0.0047$, which still implies an abrupt change in the ionization of the intercalate as the stage is increased from $n=2$ to $n=3$.

We found further support for the identification of the orbits made here on the basis of the DL model in the low-temperature specific-heat data reported by Alexander *et al.*[4] According to Alexander, if a GIC molar weight (G_{mw}) is defined by the relation

$$G_{mw}=(A_A+A_B+xA_C)/(2+x)$$

corresponding to the chemical formula C_xAB, where A_Q denotes the atomic weight corresponding to element Q, then the electronic components of the specific heat γ in stages 1 and 2 are 0.95 and 0.42, respectively, in units of (mJ/mol K^2). If we ignore the electron-phonon enhancement factor, the density of states at the Fermi surface per atom per electron volt is given by

$$N(E_F)=0.424\gamma(2+4n)\,,$$

where $(2+4n)$ is the number of atoms per formula unit. This expression for the density of states per atom consists of contributions from both the intercalate density of states (assuming that the intercalate is not completely ionized) and the graphitic density of states. On the basis of the DL model proposed for the Fermi surface in KHg_x-GIC's, we have estimated the density of states attributed to graphitic carriers at the Fermi level. A comparison with the results reported in Ref. 4 is given in Table II. The results can be interpreted to show that the ionized intercalate layer *does* contribute significantly to the electronic specific heat at least for the $n \leq 3$ compounds. This result is consistent with observations[26] in stage-1

TABLE II. Comparison between the density of states derived from the low-temperature heat-capacity data (Ref. 4), and the results of the Dresselhaus and Leung model (Ref. 8) for GIC's. By subtracting the graphitic density of states from the value measured in Ref. 4, an estimate for the intercalate density of states is obtained. Values for the charge transfer per carbon atom f_C and the Fermi level E_F, calculated on the basis of the model, are included.

			$N(E_F)/10^{20}$	
Stage	f_C	E_F	Expt[a]	DL Model[b]
1	−0.063	1.53	226	16.0
2	−0.049	1.0	63	21.0
3	−0.034	0.32		7.6

[a]Reference 4.
[b]Reference 8.

C_8K, another superconducting GIC, for which the occurrence of superconductivity requires occupation of both graphite and intercalate bands.[7]

It should be pointed out that the DL model in its simplest form deals only with graphite π-electron states. It does *not* consider any in-plane zone-folding effects. A simple geometrical argument indicates that any orbit with a period >1200 T should be affected by in-plane zone folding. Furthermore, the model also does not consider any extremal cross sections of Fermi surface associated with intercalate states (i.e., *s*, *p*, or *d* states associated with K or Hg). Since some intercalate states in these compounds are almost certainly occupied, there should be Fermi-surface cross sections associated with these electronic states. The effective-mass determination also yields information on the identification of the electronic state, since intercalate states would have very different effective masses than those which can be calculated for π bands.

CONCLUSIONS

In summary, we have performed magnetoresistance measurements on stage-1, -2, and -3 graphite potassium-amalgam intercalation compounds using the Shubnikov–de Haas effect to study the Fermi surface of these novel superconductors. The results show that the Fermi surface is stage dependent, exhibiting frequencies larger than 1000 T, and generally characterized by a highly anisotropic topography. The experimental results have been interpreted on the basis of the phenomenological model due to Dresselhaus and Leung.[8] In this application of the model, we have deduced from the SdH data that the intercalate is not completely ionized with charge transfer values consistent with the results of Conard *et al.*,[24] although the number and position of the frequencies predicted by the model are not in quantitative agreement with experiment. It is also evident by comparing the density of states obtained from the DL model with low-temperature heat-capacity measurements performed by Alexander *et al.*[4] that the intercalate contributes significantly to the density of states at the Fermi level for stages 1 and 2. The simple DL model gives only qualitative information on the electronic structure. A more exact calculation of the electronic band structure in these compounds would greatly assist the interpretation of the experimental results on the Shubnikov–de Haas effect.

ACKNOWLEDGMENTS

We wish to thank Professor M. S. Dresselhaus for many helpful discussions, and we also thank Dr. P. Tedrow, Dr. B. Brandt, and Dr. L. Rubin for the Francis Bitter National Magnet Laboratory for technical assistance. The HOPG used in these studies was kindly supplied by Dr. A. W. Moore, and the kish graphite was kindly supplied by Professor Suematsu and Professor Tsuzuku. Financial support was provided by U. S. Air Force Office of Scientific Research Contract No. F49620-83-C-0011.

[1]M. S. Dresselhaus and G. Dresselhaus, Adv. Phys. 30, 139 (1981).

[2]G. Timp and M. S. Dresselhaus, J. Phys. C (to be published).

[3]Y. Iye and S. Tanuma, Phys. Rev. B 25, 4583 (1982); Solid State Commun. 44, 1 (1982); Y. Iye, in *Intercalated Graphite,* edited by M. S. Dresselhaus, G. Dresselhaus, J. E. Fischer, and M. J. Moran (Elsevier, New York, 1983) [Mater. Res. Soc. Symp. 20, 185 (1983)].

[4]M. G. Alexander, D. P. Goshorn, D. Guérard, P. Lagrange, M. El Makrini, and D. G. Onn, Solid State Commun. 38, 103 (1981).

[5]G. Timp, B. S. Elman, M. S. Dresselhaus, and P. Tedrow, in *Intercalated Graphite,* edited by M. S. Dresselhaus, G. Dresselhaus, J. E. Fischer, and M. J. Moran (Elsevier, New York, 1983) [Mater. Res. Soc. Symp. 20, 201 (1983)].

[6]L. A. Pendrys, R. Wachnik, R. L. Vogel, P. Lagrange, G. Furdin, M. El Makrini, and A. Hérold, Solid State Commun. 38, 677 (1981).

[7]R. Al-Jishi, Phys. Rev. B 28, 112 (1983).

[8]G. Dresselhaus and S. Y. Leung, Solid State Commun. 35, 819 (1980); S. Y. Leung and G. Dresselhaus, Phys. Rev. B 24, 3490 (1981).

[9]L. G. Johnson and G. Dresselhaus, Phys. Rev. B 7, 2275 (1973).

[10]A. Hérold, D. Billaud, D. Guérard, P. Lagrange, and M. El Makrini, in *Physics and Chemistry of Layered Materials,* Proceedings of the Yamada Conference IV, edited by Y. Nishina, S. Tanuma, and H. W. Myron (North-Holland, New York, 1980), p. 253; P. Lagrange, M. El Makrini, D. Guérard, and A. Hérold, Physica 99B, 473 (1980); M. El Makrini, Ph.D. thesis, University of Nancy, France.

[11]A. Erbil, G. Timp, A. R. Kortan, R. J. Birgeneau, and M. S. Dresselhaus, Synth. Met. 7, 273 (1983).

[12]L. Salamanca-Riba, B. S. Elman, M. S. Dresselhaus, and T. Venkatesan, in Ion Implantation and Ion Beam Processing of Materials, edited by G. K. Hubler, C. W. White, C. R. Clayton, and O. W. Holland (North-Holland, New York, 1984) [Mater. Res. Soc. Symp. 27, (1984)].

[13]H. H. Sample, B. L. Brandt, and L. G. Rubin, Rev. Sci. Instrum. 53, 1129 (1982).

[14]H. C. Montgomery, J. Appl. Phys. 42, 2971 (1971).

[15]D. E. Soule, J. W. McClure, and L. B. Smith, Phys. Rev. A 134, 453 (1964).

[16]G. N. Kamm, J. Appl. Phys. 49, 5951 (1978).

[17]I. M. Lifshitz and A. M. Kosevich, Zh. Eksp. Teor. Fiz. 29, 730 (1955) [Sov. Phys.—JETP 2, 636 (1956)].

[18]R. G. Chambers, Proc. Phys. Soc. London, Sect. A 272, 192 (1963).

[19]D. Shoenberg, Philos. Trans. R. Soc. London, Ser. A 255, 85 (1962).

[20]R. S. Markiewicz, Phys. Rev. B 28, 6141 (1983).

[21]M. Shayegan, M. S. Dresselhaus, and G. Dresselhaus, Phys. Rev. B 25, 4157 (1982).

[22]K. Higuchi, H. Suematsu, and S. Tanuma, J. Phys. Soc. Jpn. 48, 1532 (1980).

[23]G. B. Brandt and J. A. Rayne, Phys. Rev. 148, 644 (1966); C. J. Palin, Proc. R. Soc. London, Ser. A 329, 17 (1972).

[24]J. Conard, H. Estrade-Szwarckopf, P. Lauginie, M. El Mak-

rini, P. Lagrange, and D. Guérard, in Physics and Chemistry of Layered Materials, Proceedings of the Yamada Conference IV, edited by Y. Nishina, S. Tanuma, and H. W. Myron (North-Holland, New York, 1980), p. 290.

[25]J. Blinowski, H. Nguyen, C. Rigaux, J. P. Vieren, R. LeToullec, G. Furdin, A. Hérold, and J. Mélin, J. Phys. (Paris) 41, 47 (1980).

[26]T. Inoshita, K. Nakao, and H. Kamimura, J. Phys. Soc. Jpn. 43, 1237 (1977); T. Ohno, K. Nakao, and H. Kamimura, *ibid.* 47, 1125 (1979).